On the lack of InSAR observations of magmatic deformation at Central American volcanoes

S. K. Ebmeier,[1,2] J. Biggs,[2,3] T. A. Mather,[1] and F. Amelung[3]

Received 14 August 2012; revised 5 April 2013; accepted 19 April 2013; published 28 May 2013.

[1] A systematic survey of 3 years of L band interferometric synthetic aperture radar (InSAR) measurements of the Central American Volcanic Arc shows a striking lack of magmatic deformation. We make measurements at 20 of the 26 historically active volcanoes and demonstrate that none were deforming magmatically (2007–2010), although we do measure shallow subsidence associated with flow deposits and edifice loading at three volcanoes. The minimum detection rates for our survey, as estimated from the variance in time series of radar path delay, are relatively high due to strong variability of tropospheric water vapor. We compare the average detection threshold (2.4 cm/yr) to published InSAR measurements and show that the majority (~78%) of deformation events would have been measurable with the same level of noise as Central America. We calculate that if magmatic volcano deformation were spread evenly across historically active volcanoes worldwide, the probability of none of Central America's 26 volcanoes deforming would be $< 1\%$. The lack of magmatic deformation in Central America may be indicative of differences in magma storage relative to other well-studied continental arcs. The high proportion of basalts that ascend directly from depth relative to andesites stored in the shallow crust may limit the potential for high magnitude deformation. Magma stored in vertically elongated reservoirs and high parental melt volatile contents that result in bubble-rich, compressible magmas at shallow depths may also reduce surface deformation. We consider the measurement and analysis of a lack of deformation at active volcanoes to be essential for realizing the potential of regional scale InSAR surveys.

Citation: Ebmeier, S. K., J. Biggs, T. A. Mather, and F. Amelung (2013), On the lack of InSAR observations of magmatic deformation at Central American volcanoes, *J. Geophys. Res. Solid Earth*, *118*, 2571–2585, doi:10.1002/jgrb.50195.

1. Arc Scale Interferometric Synthetic Aperture Radar (InSAR) Surveys

[2] The development of satellite based Interferometric Synthetic Aperture Radar (InSAR) has allowed volcano deformation to be measured at a continental scale [e.g., *Pritchard and Simons*, 2004a; *Fournier et al*., 2010; *Philibosian and Simons*, 2011; *Biggs et al*., 2011; *Chaussard and Amelung*, 2012] (see Table 2 and Supplementary Tables 1–2). InSAR uses the difference in phase between two time-separated radar images to measure small displacements of the Earth's surface at a precision of up to a few millimeters (comprehensive reviews of InSAR techniques are given by *Massonnet and Feigl* [1998] and *Bürgmann et al*., [2000]).

[3] Deformation has now been detected with InSAR at over 100 volcanoes worldwide, with marked differences between the number of observations of deformation at different volcanic arcs [*Fournier et al*., 2010], which are not obviously related to the number of historically active volcanoes. This disparity may be the consequence of both differences in the applicability of InSAR measurement under different environmental conditions and differences in magmatic processes. The extraction of information about deformation from differential phase requires the identification of phase shifts from other sources, including variations in tropospheric water vapor, differences in satellite viewing geometry and scattering properties of the Earth's surface.

[4] Environmental conditions that affect InSAR measurement vary systematically between different parts of the world. In Central America, several contributors to interferometric phase are of especially high magnitude [*Ebmeier et al*., 2013]. For example, tropospheric water vapor has both higher magnitude and greater variability in the tropics than in equatorial zones [e.g., *Heleno et al*., 2010]. Dense, rapidly growing vegetation also limits the use of InSAR measurements.

[5] In this paper, we describe the results of an InSAR survey of the Central American Volcanic Arc (CAVA), using images from the Advanced Land Observing Satellite

Additional supporting information may be found in the online version of this article.

[1]Centre for the Observation and Modelling of Earthquakes and Tectonics, Department of Earth Sciences, University of Oxford, Wellington Square, Oxford, UK.
[2]Centre for the Observation and Modelling of Earthquakes and Tectonics, School of Earth Sciences, University of Bristol, Bristol, UK.
[3]RSMAS, University of Miami, Miami, Florida, USA.

Corresponding author: S. K. Ebmeier, Centre for the Observation and Modelling of Earthquakes and Tectonics, School of Earth Sciences, University of Bristol, Bristol BS8 1RJ, UK. (sk.ebmeier@bristol.ac.uk)

2169-9313/13/10.1002/jgrb.50195

Table 1. Survey Results for Active Volcanoes in Central America

Volcano	Track/Frame	No. of Interferograms[a]	Activity During Survey	Detection Threshold (cm/yr)	Survey Result
Santiaguito	174/280	17	weak-moderate explosions, ash plumes (≤5 km), short pyroclastic flows, block and ash avalanches, lava flows, lahars	1.6	lava subsidence[b]
Almolonga	174/280	17	none (geothermal field)	0.8	no deformation
Atitlán	173/280 480/3330	17	none	4.2	no deformation
Acatenango	173/280 480/3330	11	none	5.1	no deformation
Fuego	173/280 480/3330	11	intermittent moderate strombolian, pyroclastic flows, lava flows, ash plumes (≤6 km)	5.1	no deformation
Pacaya	172/270 479/3330	24	multiple semi-continuous lava flows and intermittent strombolian activity, ash and fumerolic plumes (≤1 km)	3.0	no deformation
Santa Ana	171/260	15	lahars, intense fumerolic activity about crater lake	6.2	no deformation
Izalco	171/260	15	none	1.0	no deformation
San Salvador	170/250 474/3350	20	none	1.7	no deformation
Ilopango		0	none	–	inconclusive: poor coherence
San Miguel	168/250 474/3350	20	elevated seismicity, fumerolic	2.4	no deformation
Cosigüina	167/240-250	14	none	2.2	no deformation
Conchagüita	167/240-250	14	none	2.6	no deformation
San Cristóbal	166/230-240 472/3370	36	VEI 1 (8.11.07, 22.06.08, 21.11.08) and VEI 2 (6.9.09). Ash plumes (≤9 km)	2.7	no deformation
Telica	166/230-240 471/3370	36	VEI 1 (28.10.08,5.7.08) small phreatic explosions, ash plumes (≤2 km), minor ash explosions, incandescence in crater	1.8	no deformation
Cerro Negro	166/230-240 471/3370	36	none	1.4	no deformation
Las Pilas	166/230-240 471/3370	36	none	1.4	no deformation
Masaya	165/220-230 470/3380	20	lava lake, VEI 1 (18.6.08), intermittent ash eruptions, phreatomagmatic eruption, steam and ash plumes	1.3	subsidence within ring fault[c]
Momotombo	165/230 166/230 471/3370	49	fumerolic/geothermal	0.6	no deformation
Concepción	164/200	20	VEI 1 (9.2.07, 30.6.08, 11.12.09) and VEI 2 (24.11.07) explosions, gas and ash plumes (≤1 km)	–	inconclusive: poor coherence
Rincón de la Vieja	164 220-230	11	low level fumerolic and seismic activity	–	inconclusive: poor coherence
Miravalles	164 220-230	11	none	–	inconclusive: poor coherence
Arenal	163/190 466/3410 467/3410	12	small explosions, occasional pyroclastics	1.2	flank slip[d]
Poás	162/190 466/3410	18	VEI 1 (13.1.08, 12.1.09 and from 11.2009), phreatic explosions, fumerolic activity, landslides	0.9	no deformation
Irazú	161/180 465/3420	15	minor fumerolic	–	inconclusive: poor coherence
Turrialba	161/180 465/3420	15	increase in degassing and seismic activity preceded a VEI 2 eruption (5.1.10-24.7.10)	–	inconclusive: poor coherence

[a]Number of interferograms refers to the number processed and used during any stage of analysis, the numbers used in time series generation were sometimes lower due to variable coherence and difficulties in unwrapping.
[b](*Ebmeier et al*., 2012).
[c](*Caravantes et al*., in preparation).
[d](*Ebmeier et al*., 2010).

(ALOS) satellite, which has provided a significant set of radar data capable of penetrating tropical vegetation (2007–2010). In order to understand the significance of our measurements, we produce time series of radar path delay for 20 historically active volcanoes and calculate a minimum radar detectable rate for deformation at each (section 2.1). We then discuss the implications of the lack of measurable deformation at volcanoes that erupted during our survey (sections 4.1 and 4.2). Comparison of minimum detection rates with the magnitudes of deformation measured by InSAR at other well-studied volcanic arcs (Kamchatka, Aleutians/Alaska, Cascades, Mexico, Andes, Italy, Greece, and Sumatra/Java) suggests that the apparent lack of deformation in Central America is not primarily the result of measurement artefacts (section 5). In section 5.1, we discuss some of the factors that may limit the geodetic expression of shallow magma movement in Central America.

2. Systematic Survey of Central America

[6] We used the first significant set of radar data capable of penetrating tropical vegetation (L band, ALOS Phased Array type L band Synthetic Aperture Radar, PALSAR) to search for volcano deformation in Central America between 2007 and 2010. Earlier InSAR surveys of Central America did not detect any volcano deformation but were limited in scope by the poor coherence of C band data [*Zebker et al*., 2000] and the limited quantity of L band data analyzed in broader survey mode [*Fournier et al*., 2010].

[7] We were able to construct an average of ~15 ascending interferograms for each historically active volcano and supplemented this with descending data where possible. The Repeat Orbit Processing software (ROI_PAC) [*Rosen et al*., 2004] was used to construct interferograms, which were unwrapped using a branch-cut algorithm [*Goldstein et al*., 1988]. Topographic correction was carried out using NASA's Shuttle Radar Topography Mission 90 m digital elevation model, interpolated, and resampled to a spacing of 30 m.

[8] Interferograms showing all Central American volcanoes were examined visually for anomalous phase patterns, while phase around historically active volcanoes was scrutinized in more detail (Figure 3) (our systematic approach is set out as a flowchart in *Ebmeier et al*. [2013]). Results were considered inconclusive where fewer than three interferograms were coherent over the volcano's edifice, so that phase changes due to deformation and atmospheric water vapor could not be distinguished. At volcanoes where we had sufficient numbers of coherent interferograms, we examined the relationship between phase and perpendicular baseline separation to test for artefacts introduced by errors in the digital elevation model used in processing. We then used pairwise logic [e.g., *Massonnet and Feigl*, 1995], stacking [e.g., *Pritchard and Simons*, 2004a], and time series [e.g., *Lundgren et al*., 2001; *Berardino et al*., 2002] to examine the temporal and spatial properties of phase and to distinguish between atmospheric delays and deformation.

[9] Time series of radar path delay were constructed using a least squares approach [e.g., *Lundgren et al*., 2001], where the minimum constraint was applied to velocity rather than displacement [e.g., *Berardino et al*., 2002]. It was explicitly assumed that no deformation was taking place on the first acquisition date so that displacements were calculated relative to this date. Figure 1 shows line of sight radar delay for the coherent area surrounding the volcano summits. This is calculated relative to the average delay for an annulus centered on the volcano with radii chosen to encompass as large a continuously coherent area as possible without including topographic features associated with the volcano being studied (average inner radius 5–6 km). Referencing to the average of an area rather than an individual pixel minimizes the impact of atmospheric variation at a reference point, so that time series reflect just the differences between path delay over the volcano itself relative to the rest of the interferogram. Where phase coherence is discontinuous surrounding a volcano, we may lack a far-field unaffected by volcano deformation. This means that deep sources of deformation that produce displacements of long spatial wavelength can be harder to detect with InSAR, especially where deformation rates are low. Uncertainties in the time series were found using a Monte Carlo approach, where randomly generated atmospheric noise of mean amplitude 1 cm was added before inversion, neglecting the effects of spatial correlation. Error bars in Figure 1 therefore primarily reflect how well each acquisition date is linked to the rest of the network. Gaps in the time series where it was not possible to link independent groups of interferograms are shown in Figure 1 as gray bars.

2.1. Systematic Approach to Deformation Reporting

[10] Most InSAR papers publish details of deformation signals but do not comment on volcanoes where no deformation was observed. To make a meaningful comparison between volcanic arcs, it is vital to distinguish between volcanoes with good quality data but that were not deforming and those at which data quality were too poor for any measurement to be made. We therefore conduct a systematic survey of all volcanoes in the region, defining the limits of detectability at each.

[11] The duration of a deformation event measurable with InSAR is limited by the spacing of radar acquisition dates, while its magnitude is limited by the contributions of other sources of phase change and the total length of the period of observation. In Central America, the greatest contributions to differential phase come from variations in stratified water vapor [*Ebmeier et al*., 2013].

[12] The temporal resolution of our data (46 days at best) is low enough that we do not expect to observe "recoverable" deformation, where the ground deforms and then returns to its original position [e.g., *Watson et al*., 2000; *Dzurisin*, 2003]. The ALOS data have large gaps (up to almost 18 months for Track 173, Figure 1) and are generally irregularly spaced through time. We therefore limit ourselves to the consideration of deformation causing "permanent" change to the Earth's surface.

[13] Deformation can be identified in a single interferogram if it either (a) significantly exceeds the magnitude of atmospheric noise (δ) or (b) is spatially distinctive from atmospheric phase features. Where deformation results in permanent change to the ground, signal-to-noise ratio can be improved by "stacking" interferograms together [e.g., *Biggs et al*., 2007]. A stack of N-independent interferograms is expected to have $\sqrt{N}$ more noise than any individual image ($\delta_{stack} = \delta_{ifgm}\sqrt{N}$). Examples of stacks of interferograms from Nicaragua are presented in Supplementary Figure 1, and several individual interferograms from this data set are shown in *Ebmeier et al*. [2013].

[14] We use the root mean square variation of our time series (e.g., Figure 1) as an approximation of the typical magnitude of atmospheric noise in an interferogram or sum of consecutive interferograms (where the atmospheric contributions of dates appearing in consecutive interferograms cancel out). This value reflects the variance in radar path delay over the volcano summit relative to the rest of each interferogram and thus captures the atmospheric variability better than an average of maximum variances for full interferograms. The minimum detection rate for each volcano is then $\left(\delta_{ifgm}\sqrt{N}\right)/\ t$, where N is the number of independent chains of interferograms, and t is the total time spanned by all of the interferograms used.

3. Results

[15] Of the 26 historically active volcanoes in Central America [*Venzke et al*., 2002], we were able to make measurements at 20 (77%) (Table 1). Interferograms covering the remaining six, Ilopango, Concepción, Rincón de la Vieja, Miravalles, Irazú, and Turrialba, are not sufficiently coherent.

[16] We observed two volcanoes in the CAVA deforming as a result of loading processes: steady, downslope movement of young lavas at Arenal, Costa Rica between 2005 and 2009 [*Ebmeier et al*., 2010] and the subsidence of young lavas at Santiaguito lava dome in 2009–2010 [*Ebmeier et al*., 2012]. We also detected a region of slow subsidence at Masaya, Nicaragua, confined to a ring fault system identified through ground-based geophysical surveys [G. Caravantes et al., Structures controlling volcanic activity within Masaya Caldera, submitted to *Bulletin of Volcanology*, 2013]. Although deformation due to loading may mask low magnitude displacements of similar spatial pattern, we expect magmatic deformation to have a longer spatial wavelength and smoother shape than loading signals. We see no evidence of magmatic deformation between 2007 and 2010 in the coherent regions surrounding Masaya, Santiaguito, and Arenal (although our ability to detect long wavelength deformation is limited by interferometric coherence in some cases) [e.g., *Ebmeier et al*., 2013].

[17] A selection of apparent deformation time series for the summit areas of historically active volcanoes is presented in Figure 1. At volcanoes where data were coherent, we examined the temporal development of the apparent deformation signal to distinguish between characteristics typical of water vapor and those potentially caused by deformation. Some volcanoes (e.g., Santa Ana, Figure 1g) show "jumps" in apparent displacement associated with particular satellite images. Although conceivable that this is a rapid, reversible displacement, as the feature is associated with just one image, it is much more likely to be caused by unusual levels of water vapor at the time the radar image was acquired. Such high magnitude water vapor artefacts have commonly been observed at large volcanic edifices (Table 1) [*Ebmeier et al*., 2013]. A lack of systematic temporal structure in apparent displacement (e.g., Figures 1k and 1l) is also indicative of varying levels of water vapor [e.g., *Ebmeier et al*., 2013].

[18] The similarities between the temporal development of apparent displacement at Atitlán, Fuego, and Acatenango (Figures 1 c, 1d, and 1e) and, to a lesser extent, Izalco and Santa Ana (Figures 1f and 1g) are indicative of stratified water vapor and also illustrate the high hydrological loading on the easternmost volcanoes in Guatemala and El Salvador. A correlation between phase delay (water vapor concentration) and topographic height commonly leads to volcanoes of similar edifice height showing similar radar path delays. It also leads to a correlation between apparent displacement time series variation and edifice height (discussed further in *Ebmeier et al*. [2013], interferometric phase-topography relationships are discussed by *Remy et al*. [2003]; *Elliott et al*. [2008]). Where water vapor is persistently stratified, interferometric phase may be highly coupled for volcanoes constructed from the same set of SAR images. Although we have not attempted to do so here, in such circumstances, it may be possible to use the commonalities in phase variation at different spatial locations to remove atmospheric contributions from a time series.

[19] Our estimations of detection thresholds presented in Table 1 and Supplementary Table 3 vary between 0.6 cm/yr (at Momotombo, Nicaragua) and 6.2 cm/yr (at Santa Ana, El Salvador), with an average value of 2.4 cm/yr. High thresholds for detection are associated with low numbers of interferograms (shorter total time covered by data) and with high magnitudes of stratified water vapor artefacts over the larger volcanic edifices (e.g., at Atitlan, Acatenango, Fuego, and Santa Ana).

[20] Of the 20 historically active volcanoes in Central America where InSAR measurement was possible, we demonstrate that 10 (~50%) did not deform permanently above a rate of 2 cm/yr and 16 did not deform above a rate of 5 cm/yr (~80%) between 2007 and 2010. No evidence of deformation associated with magma movement was found.

4. Comparison to Eruptive Record

[21] In total, 14 of the 26 historically active volcanoes in Central America exhibited some level of activity between 2007 and 2010, including periods of lava effusion (e.g., Pacaya), strombolian activity (e.g., Fuego, Arenal), high flux degassing (e.g., Masaya), and fumerolic activity (e.g., Santa Ana, San Miguel). Five volcanoes had minor explosive eruptions during the period of our observations (Figure 1, marked as San Cristóbal, Telica, Masaya, Concepción, and Poás). A summary of activity from 2007 to 2010 is outlined in Table 1.

[22] Instances of eruptions where deformation is not observed are underreported in the InSAR literature, but a summary of explosive events where no deformation was measured is presented in Supplementary Table 4 and includes eruptions of similar and higher explosive index than those that occurred during our survey.

[23] There were few reports of deformation at any of Central America's volcanoes during our period of observation (2007–2010), with the notable exception of tiltmeter and leveling measurements of a potential inflation (2007) and subsequent deflation (early 2008) at Turrialba, Costa Rica, associated with the development of new fumerolic vents [e.g., *Martini et al*., 2010; *Smithsonian Institution*, 2008]. As our InSAR data were almost entirely incoherent in the area surrounding Turrialba, comparison with these data did not allow us to refine our estimations of detection threshold. Broadband seismometers have been used to measure cycles of recoverable, near-vent deformation at Fuego (tilt begins ~ 25 min before explosion) [*Lyons et al*., 2012] and Santiaguito (eruptive cycle of ~ 1 h) [*Sanderson et al*., 2010] at both temporal resolution higher and magnitudes lower than those recoverable from our InSAR data.

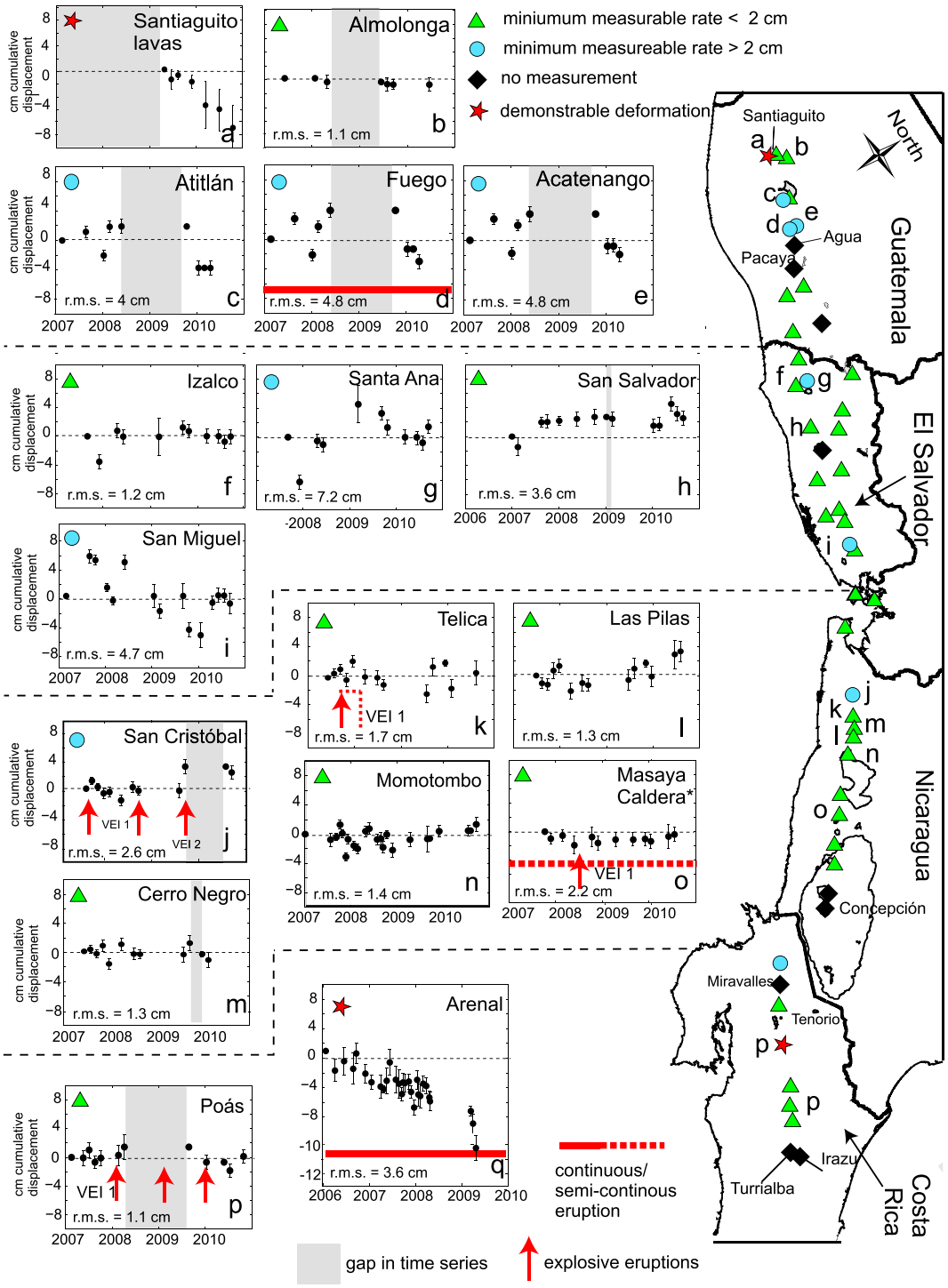

Figure 1. Summary of InSAR survey results from Central American volcanoes. Apparent displacement time series (a–q) are shown for the average path delay over summit regions of historically active volcanoes. The time series for Masaya (*) shows the average for inside Masaya Caldera, rather than the region within the ring fault, as described in *Caravantes et al*. [in preparation]. The deformation time series shown for the Santiaguito lavas was constructed after the removal of a component of phase caused by major topographic change [*Ebmeier et al*., 2012], while that for Arenal includes C band RadarSat data that allows us to extend the time series back into 2005 [*Ebmeier et al*., 2010]. The activity of these volcanoes during the period of InSAR survey is described in Table 1. Explosive eruptions are marked by red arrows, and gaps in the time series are shown as gray boxes. "r.m.s." refers to the root mean square variability of the detrended time series, as described in section 2.1. All the volcanoes investigated using the time series approach described in section 2.1 are listed in Table 1.

[24] Previous ground based measurements of deformation in Central America seem predominantly to have captured low-magnitude, spatially limited signals. For example, one dry tilt instrument 1 km South of Poás' crater has shown a general trend of subsidence since measurements began in 1989 (~ 6 μrad/yr) [*Smithsonian Institution*, 1993a, 1993b] but electronic distance meter measurements made across the volcano summit have not detected significant changes [e.g., *Smithsonian Institution*, 1993a, 1993b, 2000]. Similarly, leveling measurements across Irazú's crater area captured a period of expansion in 1991–1992 (horizontal expansion rate of 1.3 cm/yr) [*Smithsonian Institution*, 1993c]. Repeat elevation measurements at gravity stations in Masaya caldera between October 1994 and September 2001 recorded variations in height of average standard deviation 3.6 cm/yr [*Williams-Jones et al*., 2003], but these measurements show no systematic trends consistent with large-scale inflation or deflation, and it is unclear whether they would allow the identification of either short-lived or localized deformation (such as that we observe within Masaya's ring fault). In contrast, *Eggers* [1983] measured deflation of up to 20 cm at Pacaya in 1979–1980, magnitudes that would have been well above our InSAR detection limits had a similar episode occurred between 2007 and 2010.

4.1. Explosive Eruptions

[25] The mechanism by which an explosive eruption is driven determines the character of deformation, if in fact any deformation occurs. For example, rapid cycles of inflation and deflation can be driven by conduit pressurization building up beneath a crystallized plug before explosion (e.g., Montserrat, deformation period 6–18 h) [*Voight et al*., 1999]. Even more rapid deformation cycles are associated with the growth of bubbles and ascent of mafic magma in an open conduit (e.g., Stromboli, deformation period ~ 250 s) [*Genco and Ripepe*, 2010]. In Central America, explosions at Fuego [*Lyons et al*., 2012] and Santiaguito [*Sanderson et al*., 2010] are associated with conduit pressurization processes. This deformation is beyond the temporal resolution of the ALOS data used in this study (satellite repeat time 46 days).

[26] Minor explosions associated with the clearing of a blockage in a dominantly open system are also unlikely to result in high-magnitude deformation. Explosions at Masaya have previously been attributed both to such "vent-clearing" processes and to interactions with the hydrothermal system (e.g., 23 April 2001, VEI 1) [*Duffell et al*., 2003], and the event during our measurement period (18 June 2008, VEI 1) [*Smithsonian Institution*, 2009] is expected to have been similar in character. Phreatic eruptions at Poás in 2008 and 2009 may have been associated with similar processes. Recent deployment of continuous GPS at Telica allowed measurement during a series of ash explosions in May 2011 and showed little deformation [*Witter et al*., 2011]. The nonjuvenile composition of the ash from these explosions combined with the lack of deformation suggests that this eruption was amagmatic. If the similarly explosive eruptions at Telica and San Cristóbal during 2007 and 2008 were similar in character to this eruption, then it seems likely that there was no significant coeruptive deformation associated with these events. Although there is an intriguing uplift of ~ 4 cm at San Cristóbal in August 2009, this feature is associated with just one acquisition date. As we were unable to construct any interferograms spanning the time between 16 September 2009 and 4 August 2010, we are unable to examine the temporal structure of this signal and perform tests that would allow us to confidently identify it as deformation rather than water vapor artefact.

[27] The majority of coeruptive deformation events measured with InSAR to date have captured the accumulation, emptying, and/or recharge of a reservoir, most commonly at depths above 5 km and almost all above 10 km depth (Table 2 and Supplemental Tables 1 and 2). Many examples of deformation accompanying dyke intrusion (Table 2) and a few instances of conduit processes or summit caldera subsidence (e.g., at Lascar and Colima) [*Pavez et al*., 2006; *Pinel et al*., 2011] have also been captured by InSAR measurement.

[28] A comparison of the explosive eruptions covered by our survey (Table 1) and some examples of those from the global literature that have produced measurable coeruptive deformation (Table 2) are presented in Figure 2a. We limit comparison to coeruptive deformation where it was considered reasonable to approximate the deformation source mechanism as a point. Contours of equal surface displacement for a point source in a uniform elastic half space [*Mogi*, 1958] are marked in Figure 2 in red. The range of deformation detection limits found for Central American explosions (at San Cristóbal, Telica, Masaya, and Poás) is indicated by an orange bar. The potential range of positions for the 2007–2008 Central American explosions is shown as a gray box in Figure 2a and is based on the assumption that any associated volume change was less than 10^{-4} km^3, the maximum volume change expected for a VEI 2 eruption. Even if explosions at San Cristóbal, Poás, and Telica (2007–2009) were associated with the deflation and subsequent recharge of shallow reservoirs, differing from the 2011 Telica eruption described above, the volume changes ($<10^{-4}$ km^3) would have been among the lowest measured with InSAR (e.g., Llaima and Slamet) [*Bathke et al*., 2011; *Philibosian and Simons*, 2011].

[29] Although eruptions between 2007 and 2010 did not result in permanent deformation above the level of atmospheric noise, historical eruptions in Central America have been significantly larger. Figure 2b shows 20th century eruptions of explosivity index VEI 3 and greater. Of these larger eruptions, we expect the 1902 eruption of Santa Marìa to have produced high magnitude surface deformation (>10 cm), and Arenal's 1968 eruption (of a similar volume to eruptions where InSAR measurements have been successful at Okmok and Chaitén) [*Lu and Dzurisin*, 2010; *Fournier et al*., 2010] to have resulted in deformation of the order of a few centimeters, high enough to potentially be detectable with this study's measurement limits.

4.2. Persistent Activity

[30] Persistently active volcanoes show evidence of significant surface activity (e.g., degassing, fumerole fields, high surface temperatures) over extended periods of time, without a large associated extrusive flux [*Francis et al*., 1993]. Central American volcanoes where mass flux estimated from SO_2 degassing flux and melt inclusion sulphur content exceed effusion rate by 2 or 3 orders of magnitude include Masaya, Pacaya, and Telica. Such processes are thought to be maintained through the convective overturning of magma within a network of conduits, where

Table 2. Summary of Published InSAR Measurements of Coeruptive and Posteruptive Deformation[a]

Volcano	Max. Rate (cm/yr)	Model	Depth (km)	ΔVolume (m^3)	Reference(s)
Eruption					
Seguam	10	Mogi array	0.5–5.5	–	*Masterlark and Lu* [2004]
1992-93 VEI 2					
Okmok	2–10	Mogi	3.5	$-4.7 \pm 0.5 \times 10^7$	*Lu and Dzurisin* [2010]
1997 VEI 3					
	17–20	Mogi	3.5	$3.7–5.2 \times 10^7$	*Lu and Dzurisin* [2010]
2008 VEI 4					
Makushin	7	Mogi	7	2.2×10^7	*Lu et al.* [2002b]
1995 VEI 1					
Colima	-1.5^c	Mogi	2.5	0.23×10^6	*Pinel et al.* [2001]
97-11 dome growth					
Galeras	−3	Mogi	2	6.5×10^5	*Parks et al.* [2011]
2008 VEI 1					
Lascar	-1.7^c	Mogi	0.18	2×10^5	*Pavez et al.* [2006]
1995 VEI 2					
Llaima	-10^b, 8^a	Mogi	4-12	-10 to 46×10^{6b} $6–20 \times 10^{5a}$	*Bathke et al.* [2011]
2003,07-08 VEI 2,3					
Chaitén	−22	dyke/Mogi	15.9	$3–10 \times 10^7$	*Fournier et al.* [2010]
2008 VEI 4					
Soufrière Hills	$2–3^c$, 1–2	Mogi	6	–	*Wadge et al.* [2006]
99-00 dome growth					
Etna	?	Yang, fault	4.8		e.g., *Lundgren et al.* [2003]
1995 VEI 3					
Krakatau	4^a, $6,-9^b$	dyke	0.4	$1.05–1.08 \times 10^6$	*Agustan et al.* [2012]
2007-08 VEI 2					
Slamet	$3^{a?}$	Mogi	0.8–1.5	$3–5 \times 10^5$	*Philibosian and Simons* [2011]
2009 VEI 1					
Sinabung	$4.7^{a?}$	Mogi	0.7	–	*Chaussard and Amelung* [2012]
2010 VEI 2					
Kerinci	$6.4^{a?}$	Mogi	1.6	–	*Chaussard and Amelung* [2012]
2009 VEI 1					
Ol Doinyo Lengai	< 40	dyke, mogi, fault	4, 5.6, 3.6	–	*Biggs et al.* [2009a]
2007 rifting					
Nyamulagira	28	two dykes	0, 3	–	*Wauthier et al.* [2012]
2002 VEI 2?					
Nyiragongo	15	dyke	1–3?	–	*Wauthier et al.* [2009]
2002 VEI 2?					
Eyjafjallajökull	-	sill	4.5–4.6	$13–15 \times 10^6$	*Sigmundsson et al.* [2010]
2010 VEI 4					
Hekla	0.5	Mogi	14–20	$4–8 \times 10^4$	*Ofeigsson et al.* [2011]
2000 VEI 3					
Piton de la Fournaise	50	dyke (open 60 cm)	<1	–	*Sigmundsson et al.* [1999]
1998 VEI 1					
	30	dyke	< 1	–	*Froger et al.* [2004]
2003 VEI 1					
Kilauea	~10	dyke	5	3.3×10^6	*Cervelli et al.* [2002]
dyke intrusion, 1999					
Fogo	10	dyke	2	–	*Amelung and Day* [2002]
1995 VEI 2					
Cerro Azul	−15	Mogi	5	–	*Amelung et al.* [2000]
1998 VEI 1					
Fernandina	90	dyke	3	–	*Amelung et al.* [2000]
1995 VEI 2					

[a]We include note of best-fit analytical source model, source depth and volume change. Events marked '^{a}' were pre-eruptive, those marked '^{b}' were posteruptive. Events marked '^{c}' were limited to summit area only.

buoyant magma loses volatiles and heat to the atmosphere (or overlying hydrothermal system) and sinks to accumulate in the shallow to mid-depth crust [e.g., as described by *Locke et al.*, 2003]. The rise and fall of magma level in a rigid conduit takes place on a time scale of weeks to months (days for Strombolian activity) and is not accompanied by deformation for mafic systems where magma is of a low enough viscosity not to couple to conduit walls. Observations of such processes have been made from microgravity measurements at Telica, Poás, and Masaya and have captured changes in conduit magma level [*Rymer et al.*, 1995; *Williams-Jones et al.*, 2003; *Locke et al.*, 2003] apparently unaccompanied by large-scale deformation. The accumulation of degassed magma is therefore the only component of typical "open" system behavior expected to produce deformation.

[31] *Francis et al.* [1993] suggest that the accumulation of degassed magma may result in endogenous growth due to localized emplacement into and beneath a volcano's edifice, a process that, if shallow enough, should be detectable as deformation. It has also been suggested that magma may return to cumulate complexes at greater depths [e.g., *Locke et al.*, 2003] or be recycled in an active reservoir [*Harris et al.*, 1999]. In Central America, gravity measurements have

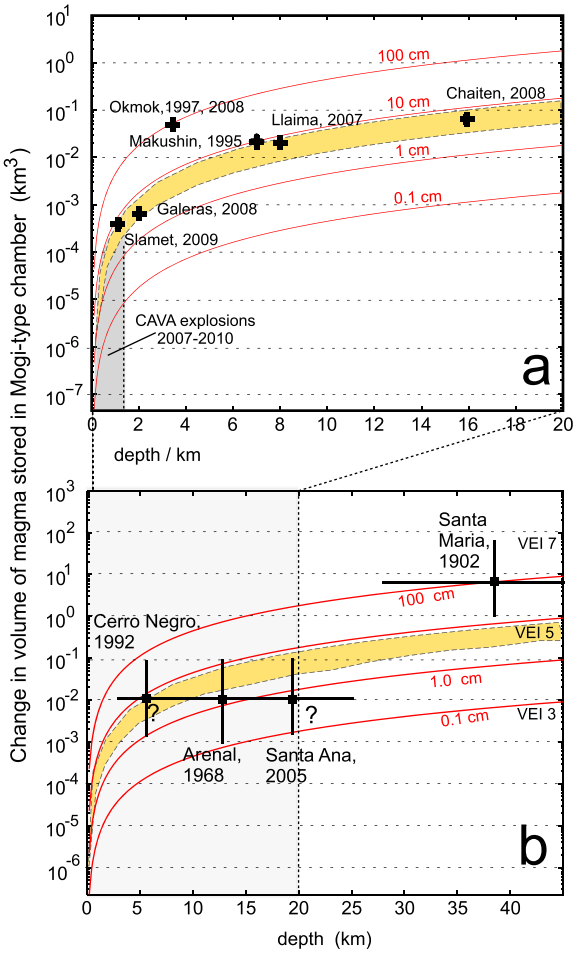

Figure 2. Plots illustrating the relationship between depths, volume changes, and deformation for explosive eruptions. Red contours show equal magnitude surface deformation for a one-dimensional model of a spherical pressure source in a uniform elastic half-space. The orange bar indicates the range of minimum deformation magnitudes (found from threshold rates, Table 1, and longest interferogram time span) for explosions during this survey. (a) Published examples of volcanoes where magma depth and volume change has been estimated from (black crosses) InSAR data. An estimated range of depths, assuming volume changes $<10^{-4}$ kg m^{-3} for explosions in CAVA (2007–2010) is marked by the gray box. References are in Table 2. (b) Large historical eruptions in Central America plotted to show their relative size (we use VEI index ± 1 as a very rough indicator of erupted volume) and presumed depths of reservoirs. Magma storage is thought to take place below ~ 6 km at Cerro Negro [*Roggensack et al.*, 1997], at 12–14 km depth at Arenal [*Pertermann and Lundstrom*, 2006], at "lower crustal" depths for Santa Maria [*Rose*, 1972] and at "midcrustal" depth at Santa Ana [*Carr*, 1981a]).

not uncovered shallow magma accumulation at Masaya or Poás, although small increases in gravity at Telica between 1994 and 2000 indicate an accumulation of material at depths below several hundred meters [*Locke et al.*, 2003].

[32] Measurements of surface deformation will be more sensitive to localized accumulation than to dispersed intrusion. We use our InSAR measurements to make an order of magnitude estimation of the depth below which localized magma accumulation could be taking place without causing measurable deformation. We estimate mass flux of degassing magma at three persistently active volcanoes from average degassing flux (Q_{SO_2}) and estimations of decrease in melt sulphur content assuming complete degassing (ΔC_S), as described by *Kazahaya et al.* [1994]. This is converted to a magma volume flux (ΔV) using an assumed magma density (ρ_m) of 2800 kg m^{-3} as follows:

$$\Delta V = \frac{M_S Q_{SO_2}}{M_{SO_2} \Delta C_S \rho_m} - Q_{\text{eff}}, \quad (1)$$

where Q_{SO_2} is average degassing flux of SO_2 [*Mather et al.*, 2006], M_S and M_{SO_2} are the molecular masses of S and SO_2, and Q_{eff} is the effused volume flux (as presented in Table 3). We estimate ΔC_S, the decrease in magma sulphur content assuming complete degassing expressed in ppm, from melt inclusion analyses [*Walker et al.*, 2003; *Sadofsky et al.*, 2008]. We choose the highest measured value for magma sulphur content (closest to parental melt concentration) in each case and assume complete degassing. The mass and volume fluxes presented in Table 3 may therefore be underestimates. Our estimation of magma mass flux at Masaya (4×10^{11} kg/yr) is of the same order of magnitude as *Stoiber et al.*'s [1986] estimate of mass flux for 1980–1982, 1.9×10^{11} kg/yr, which assumes that 75% of the magma's sulphur content is lost during degassing.

[33] We use our estimated volume fluxes in conjunction with our threshold detection rates, (V_r) for Masaya, Pacaya, and Telica (1.3, 3, and 1.8 cm/yr, respectively) to make order of magnitude estimates of minimum accumulation depth using an elastic half-space point source model (Figure 3c). Minimum depth would then be:

$$d^2_{\text{min}} = \frac{(1-\nu)}{\pi V_r} \left[\frac{M_S Q_{SO_2}}{M_{SO_2} \Delta C_S \rho_m} - Q_{\text{eff}} \right], \quad (2)$$

where V_r is threshold detection rate, and ν is Poisson's ratio.

[34] There are high uncertainties associated with our calculation of magma volume flux, primarily as a result of (1) the use of SO_2 flux (Q_{SO2}) measurements that predate our period of InSAR measurements, (2) the use of melt inclusion measurements of sulphur content (ΔC_S) that may not reflect true parental melt sulphur content, and (3) uncertainties in the effusive flux. We use the standard deviation in measurements contributing to *Mather et al.*'s [2006] 1997–2003 mean of measured SO_2 flux [e.g., *Andres and Kasgnoc*, 1998; *Duffell et al.*, 2003; *Zimmer et al.*, 2004] to approximate temporal variability in SO_2 flux. We show the effect of one standard deviation difference on our estimations of minimum depth in Figure 3. We also include estimations of depths for Masaya both made from published sulphur content and using a value of 1000 ppm in Figure 3 to illustrate the potential uncertainties introduced by choice of magma sulphur content.

[35] However, our order of magnitude estimations suggest that there is no localized magma accumulation above depths of ~ 4 km at Telica and none above depths of ~ 10 and ~ 40 km at Masaya and Pacaya, respectively. This makes the unrealistic assumption of elastic behavior down to the base of the crust, so true minimum detection depths are expected to be shallower than this.

Table 3. Selected Persistently Active Volcanoes in Central America, Where Activity Is Characterized by Open System Activity[a]

Volcano	Extrusion Rate (m^3/yr)	SO_2 flux [b] (t/d)	S Content of Melt Incl (ppm)	Mass Flux (kg/yr)	Volume Flux (m^3/yr)
Pacaya	5.3×10^{6}[c]	1540 ± 370	1680[d]	$2 \pm 0.4 \times 10^{11}$	$5 \pm 0.1 \times 10^{8}$
Telica	very low	280 ± 240	2408[e]	$2 \pm 1 \times 10^{10}$	$8 \pm 6 \times 10^{6}$
Masaya	7×10^{4}[f]	800 ± 590	385[e,g]	$4 \pm 2 \times 10^{11}$	$1 \pm 0.9 \times 10^{8}$

[a]Estimations of volume flux assume a magma density of 2800 kg m^{-3}. We use the highest values of sulphur content we could find in the literature.
[b]1997–2004 mean SO_2 flux as in *Mather et al.* [2006], uncertainties are one standard deviation in contributing measurements.
[c]1961–2001, *Durst* [2008].
[d]The highest of the values found by *Walker et al.* [2003].
[e]*Sadofsky et al.* [2008].
[f]Since 1524, *Stoiber et al.* [1986]. Extrusive flux over the past two decades has been much lower than this.
[g]*Stoiber et al.* [1986] found 320 ppm S in melt inclusions in scoria from 1981. This is very low for a basalt [e.g., *Wallace*, 2005], and is therefore probably not representative of parental melt composition. Volume flux at Masaya may therefore be a factor of ~ 3 lower than our estimates (see Figure 3).

[36] Our results, in common with gravity data [*Locke et al.*, 2003], suggest that there is no shallow, localized accumulation of magma at persistently active volcanoes in Central America. Degassed magma is therefore likely to be (a) returning to great depth and/or (b) dispersed through the mid to lower crust in a large number of individually small intrusions so that volume changes are too small to result in surface deformation. The greater the area over which degassed magma is distributed, the lower the rates of any resultant surface deformation.

5. Comparison to Other Volcanic Arcs

[37] We compare our results to published measurements of deformation at other volcanic arcs (Figure 4a), separating observations into magmatic and non-magmatic processes (such as loading effects and the deformation of flow deposits). Any statistical comparison that relies on examining the temporal distribution of InSAR deformation measurements is problematic, because observation periods are not commonly reported in the literature, especially where no deformation was measured. We therefore test the statistical significance of the lack of deformation observed in Central America with respect to the distribution of deformation at historically active volcanoes at other volcanic arcs. Our null hypothesis is that all historically active volcanoes are equally likely to deform in a manner measurable with InSAR. We use Fisher's exact test of independence [*Fisher*, 1922] to examine the probability that each arc in Table 4 is part of the global set of InSAR measurements. For our purposes, an exact test is favorable over criteria that rely on the sample distribution approximately matching a theoretical distribution (e.g., Pearson's χ^2 test) due to the small sample size (P values set out in Table 5).

[38] We do not reject our null hypothesis for non-magmatic deformation (Figure 4b), as this is distributed relatively evenly between active volcanoes. The probabilities of the observed distributions of magmatic deformation arising randomly, however, are considerably lower, and we find statistically significant (at the 95% level) deviations in the numbers of measurements of deformation in Central America, the Central Andes, and Aleutian Islands (Figure 4c). In both the Central Andes and Aleutians, the number of observations of deformation exceed the number expected per historically active volcano, while in Central America, they are significantly lower than expected. If deformation measurements were distributed evenly across the world's historically active volcanoes, the probability of none of Central America's 26 historically active volcanoes deforming in a manner measurable using InSAR would be < 0.01.

[39] An obvious concern given the different time periods of observations is that the length of time over which InSAR measurement has been possible might control the number of observations of volcano deformation at each arc. We do not think that this is the case, because arcs with exactly the same temporal coverage of InSAR measurements show a range in number of deformation measurements. Specifically, the recent availability of L band data (since 2007) has allowed the first InSAR surveys of volcano deformation to be made for Java, Lesser Sunda, Sumatra, the Northern Andes, and Central America (Figure 4, marked with a star), with the number of

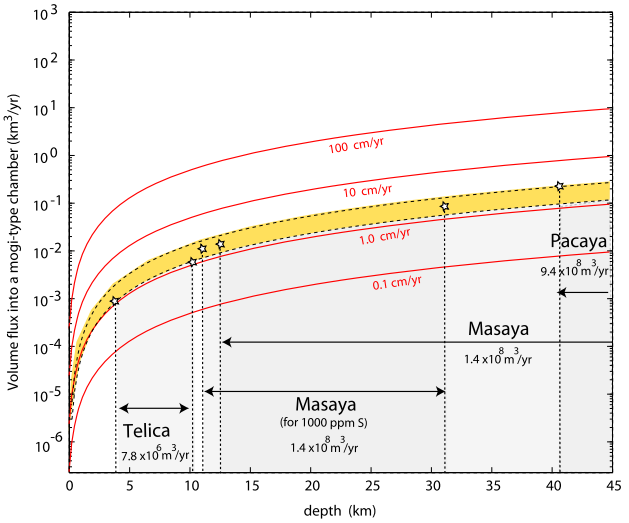

Figure 3. Estimations of the depths below which degassed magma could be accumulating in a reservoir approximated as a point source without causing measurable surface deformation. The range of threshold detection rates for Telica, Pacaya, and Masaya is indicated by the orange bar bounded by dashed lines, and peak surface deformation contours are shown in red (as for Figure 2). Estimated volume fluxes shown are derived from average SO_2 emission fluxes (1997–2003) and the sulphur content of melt inclusions (calculations are presented in Table 3). The range between upper and lower bounds on volumes, treated as one standard deviation of the SO_2 flux measurements made between 1997 and 2003, is indicated by a gray box for each volcano to give an indication of uncertainty. A lower potential volume flux for Masaya, estimated for sulphur content of 1000 ppm is included as melt inclusion measurements of sulphur content at Masaya are very low and may not reflect parental melt compositions.

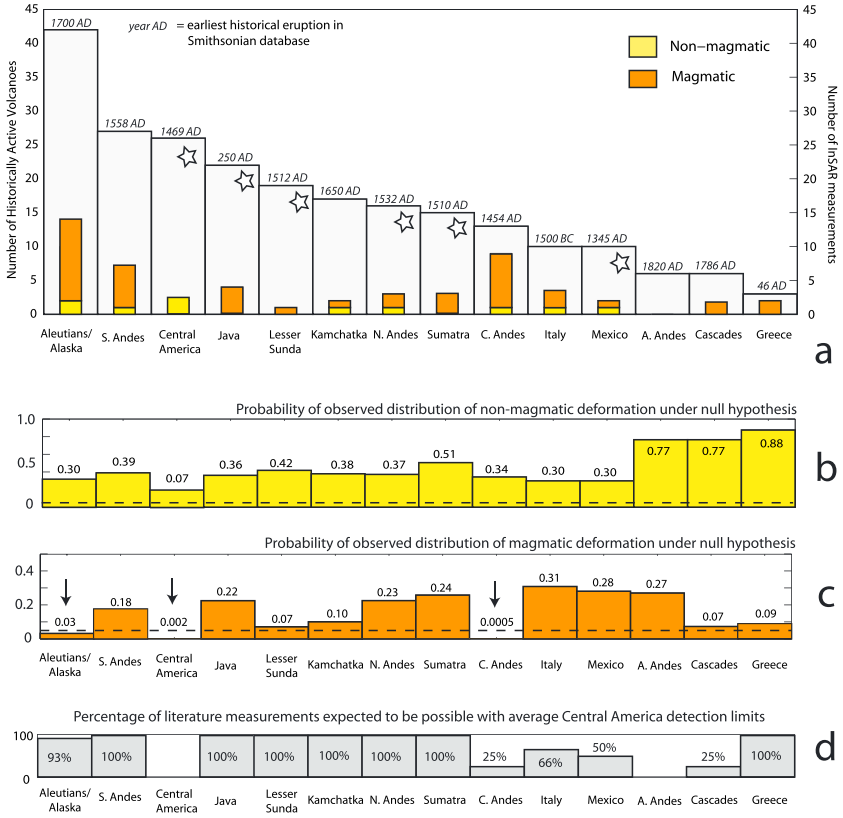

Figure 4. (a) Published InSAR measurements of volcano deformation at 14 of the best geodetically studied volcanic arcs, presented in decreasing order of the number of historically active volcanoes. The date of the first historical eruption recorded in the Smithsonian database is marked in italics at the top of each bar and bears no relationship to the number of volcanoes classed as historically active. The number of measurements of non-magmatic deformation is shown in yellow and magmatic deformation is shown in orange. White stars mark arcs where survey-type studies have been made just with ALOS data and therefore have the same temporal coverage. (b) Probabilities of the observed numbers of nonmagmatic deformation events occurring at each arc if deformation measurements were evenly spread around the world's historically active volcanoes (Fisher exact test of independence). The 95% confidence interval is shown as a dotted line. (c) Probabilities of the observed numbers of magmatic deformation events occurring at each arc if deformation measurements were evenly spread around the world's historically active volcanoes. Arcs where deviation from the expected number of deformation events is statistically significant (at the 95% level) are marked with an arrow. (d) The percentage of measurements of deformation for each arc that exceed the average magnitude of atmospheric noise at Central American volcanoes (see Table 4).

measurements of magmatic volcano deformation being 4, 1, 3, 2, and 0, respectively [*Philibosian and Simons*, 2011; *Fournier et al.*, 2010; *Biggs et al.*, 2009b; *Chaussard and Amelung*, 2012]. For these arcs, where suitable data have only been available since 2007, only Central America shows any statistically significant undersampling for magmatic deformation. As published InSAR surveys do not generally report a lack of deformation, or catalogue where measurement was possible, for the purposes of our comparison, we treat all historically active volcanoes where deformation was not reported as not deforming. We assume that the occurrence of deformation is independent of the factors that control whether or not InSAR measurement is possible. If we recalculate our statistical test with data for just the 20 volcanoes in Central America, where we were able to make InSAR measurements, the probability of not measuring magmatic deformation in Central America is about 0.02 (significant at the 95% level).

[40] This result indicates a systematic difference in the occurrence of deformation measurable with InSAR on the CAVA, relative to other well-studied arcs. We investigate whether this difference is likely to be due to particular difficulties in making InSAR measurements by comparing published deformation measurements to the average minimum measurable rate for Central America (2.4 cm/yr) (Table 4 and Supplementary Table 3). This allows us to make estimates of the approximate percentage of deformation measurements that would have been possible with similarly high levels of atmospheric noise to Central America (Figure 4d). Although the large majority of published measurements would have been possible (~80%), a slightly lower percentage of magmatic deformation events (73%) exceed our average minimum detection rate than nonmagmatic events (86%). If we repeat the Fisher tests of independence including just those deformation events that would have been

Table 4. Arc Scale Comparison of InSAR-Measured Deformation[a]

Volcanic Arc	Temporal coverage	No of volcanoes	No. of Historically Active	No. of InSAR Measurements			% > Threshold
				Magnetic	Non-magnetic	Total	
Kamchatka [b]	1992–2003	77	17	1(**1**)	1(**1**)	2(**2**)	100%
Alaska/Aleutians [c]	1992–2010?	91	42	12(**10**)	2(**2**)	14(**12**)	93%
Cascades [d]	~1992–2001	64	6	2(**1**)	0	2(**1**)	50%
Mexico [e]	1990s, 2007–2010	43	10	1(**0**)	1(**1**)	2(**1**)	50%
Central America [f]	2007–2010	**72**	**26**	**0**	**3**	**3**	-
Northern Andes [g]	2006–2010	35	16	2(**2**)	1(**1**)	3(**3**)	100%
Central Andes [h]	1992–2010	69	13	8(**2**)	1(**0**)	9(**2**)	25%
Southern Andes [i]	2002–2008	63	27	6(**6**)	1(**1**)	7(**7**)	100%
Austral Andes [j]	1996–1999	7	6	0	0	0	-
Italy [k]	~1992–2000	15	10	2(**1**)	1(**1**)	3(**2**)	66%
Greece [l]	1995–2000, 2010–2011	6	3	2(**2**)	0	2(**2**)	100%
Sumatra [m]	2007–2010	32	15	3(**3**)	0	3(**3**)	100%
Java [n]	2007–2010	39	22	4(**4**)	0	4(**4**)	100%
Lesser Sunda [o]	2007–2010	28	19	1(1)	0	1(1)	100%
% observable in Central America:				73%	86%	78%	

[a]Bold numbers in parentheses indicate the number of measurements that would have been possible with Central American limits applied. References that describe large-scale surveys are included in the table, information regarding individual volcanoes is summarized in Table 2 and Supplementary Tables 1 and 2.
[b]*Pritchard and Simons* [2004b]; *Lundgren and Lu* [2006].
[c]*Lu* [2007]; *Lu and Freymueller* [1998]; *Lu et al*. [2002a]; *Lu et al*. [2003]; *Lu and Dzurisin* [2010]; *Moran et al*. [2006].
[d]*Dzurisin et al*. [2006]; *Poland et al*. [2004]; *Poland et al*. [2006].
[e]*Fournier et al*. [2010]; *Pinel et al*. [2011].
[f]This work and *Ebmeier et al*. [2010]; *Ebmeier et al*. [2012]; *Caravantes et al*. [in prep].
[g]*Mothes et al*. [2008]; *Biggs et al*. [2010]; *Parks et al*. [2011].
[h]*Pritchard and Simons* [2004a]; *Fournier et al*. [2010]; *Sparks et al*. [2008]; *Pavez et al*. [2006]; *Froger et al*. [2007]; *Ruch et al*. [2008].
[i]*Pritchard and Simons* [2004b]; *Fournier et al*. [2010]; *Bathke et al*. [2011].
[j]*Pritchard and Simons* [2004b]; *Fournier et al*. [2010].
[k]*Lundgren et al*. [2001]; *Lanari et al*. [2002].
[l]*Sykioti et al*. [2003]; *Parks et al*. [2012].
[m]*Chaussard and Amelung* [2012].
[n]*Philibosian and Simons* [2011].
[o]*Agustan et al*. [2012]; *Chaussard and Amelung* [2012].

observable in Central America, the probability of no historically active volcanoes deforming in Central America is even lower than that shown in Figure 4b, with a P value much lower than 0.01.

Table 5. Probabilities of Observing the Number of Deformation Events Found at 14 Volcanic Arcs (as in Figure 4) According to a Fisher's Exact Test With the Null Hypothesis that Deformation Is Evenly Distributed Around the World[a]

Volcanic Arc	Nonmagmatic deformation	Magmatic deformation
Aleutians/Alaska	0.333	0.032
Southern Andes	0.397	0.175
Central America	0.198	0.003
Java	0.4012	0.225
Lesser Sunda	0.4570	0.071
Kamchatka	0.367	0.100
Northern Andes	0.359	0.225
Sumatra	0.542	0.258
Central Andes	0.326	0.0005
Italy	0.280	0.308
Mexico	0.280	0.280
Austral Andes	0.787	0.270
Cascades	0.787	0.073
Greece	0.888	0.090

[a]Each arc was compared to the rest of the global literature separately. Values for which the deviation from the null hypothesis is significant (i.e. distribution of deforming volcanoes is not spatially random) are underlined.

[41] Our analysis suggests a statistically significant difference in the number of measurements of magmatic deformation made in Central America relative to other parts of the world. As ~80% of published measurements exceed the average minimum detectable rate for Central America, this may imply some difference in the average character of magma storage.

5.1. Limiting Factors for Surface Deformation

[42] The factors that control the geodetic expression of magma movement at an individual volcano are numerous and complex. Magma flux, composition, storage depth, storage geometry, and the existence of an open conduit are all important. Although there may be general commonalities in these factors for volcanoes in the same regional setting (e.g., Table 6), local conditions may be equally significant (e.g., reservoir geometry may be affected by local stress fields). Factors affecting the occurrence of deformation may also vary along the length of a volcanic arc. In Central America, the existence of systematic along-strike variation in geochemistry and tectonic parameters are well-established [*Patino et al*., 2000; *Carr et al*., 2003; *Bolge et al*., 2009]. We therefore limit ourselves to suggesting factors that may have the potential to contribute to low geodetic expression of magma movement that are applicable across all or most of the CAVA.

[43] The CAVA has a high proportion of basalts to andesites [*Carr*, 1984] relative to other continental arcs, suggesting that more magma potentially rises directly from the base

Table 6. Summary of Physical Characteristics of Tectonic Parameters for Selected Well-Studied Segments of Volcanic Arcs[a]

Volcanic Arc	Convergence Rate[b] (Trench Normal) (mm/yr)	Extension/Compression[b] (mm/yr)	Arc-Parallel Slip[b] (mm/yr)	Volume Extrusion Rate per 100 km[b] (km^3/yr)	Modeled H_2O Flux at 100 km^2 ($Tg\ Ma^{-1}\ m^{-1)}$	Average Surface Heat Flux[d] ($mWm^{-2)}$
Kamchatka	74	10 ± 5	5 ± 3	$3 \pm 0.9 \times 10^{-3}$	25	84
East Aleutians	65	-5 ± 5	0 ± 1	$0.2 \pm 0.07 \times 10^{-3}$	19	–
Alaska (Katmai)	58	-1 ± 1	0 ± 1	$0.26 \pm 0.05 \times 10^{-3}$	15.2	77
Cascades	24	2 ± 1	0 ± 1	$0.95 \pm 0.04 \times 10^{-3}$	1.9	80
Mexico	51	0.4 ± 0.04	0.14 ± 0.01	$0.14 \pm 0.04 \times 10^{-3}$	6.1	111
Central America	73	8* and $4^{\S} \pm 2$	11 ± 2	$3.1 \pm 0.8 \times 10^{-3}$	17–21	82
Andes (Southern)	75	-1 ± 1	10 ± 8	$1.3 \pm 0.4 \times 10^{-3}$	16	79
Sumatra	41	0 ± 2	23 ± 2	$6.6 \pm 2 \times 10^{-3}$	10–12	66

[a]These arc segments do not correspond directly to the arcs shown in Figure 4, but do give an indication of nearby tectonic parameters. Extension is considered to be positive and compression negative.
[b]*Acocella and Funiciello* [2010].
[c]*van Keken et al*. [2011], fixing slab-overriding plate coupling depth at 80 km and including contributions from serpentenization [based on thermal models of *Syracuse et al*., 2010].
[d]*Zellmer* [2008].
In Central America, extension has both arc-parallel (*) and arc-normal (§) components

of the crust without a period of crustal storage. The large density contrast at the base of the Central American crust (thickness = ~25–45 km) is thought to trap basalts at depths well below those for which volume changes are commonly detected geodetically. Volume changes would have to be both localized and exceed volumes on the order of 10^7–10^9 m^3 to produce deformation of the order of 1 cm magnitude. Basalts are thought to ascend rapidly from depth during eruption (e.g., at Fuego, Guatemala or Cerro Negro, Nicaragua), with the only exception being around Masaya in Nicaragua where thinner crust allows the ascent of denser, more mafic material that becomes trapped by less dense layers in the shallow crust [*Walker*, 1993]. As basalts are at least as common as andesites in Central America, a large proportion of volcanic activity may not involve any stage of storage in the shallow crust.

[44] The compressibility of bubble-rich magma can accommodate some or even all of the volume change associated with a magmatic intrusion, so that large intrusions can result in low magnitude surface deformation [e.g., *Johnson et al*., 2000; *Mastin et al*., 2009]. This effect is most significant for pressure changes involving evolved, gas-rich magma at shallow depths [e.g., *Mastin et al*., 2008]. Conditions that affect the compressibility of a shallow magma include its temperature, time of residence in the crust (and therefore crystal content), parental melt content, and the degree of degassing, i.e., remaining exsolved gas content. In the absence of a detailed knowledge of all of these conditions, the problem of magma compressibility in Central America is underconstrained. However, if exsolved gas content at shallow depths correlates with parental melt volatile content, perhaps where little to no degassing has taken place, then the distinctively high water contents inferred for Central American parental melts [*Wallace*, 2005; *Sadofsky et al*., 2008] may result in particularly high magma compressibility.

[45] Vertically elongated magma reservoirs, thought to be common beneath stratovolcanoes, produce lower magnitude surface deformation than spherical reservoirs for the same depth and pressure change. For example, comparison of a vertically elongated ellipsoid (*Yang et al*. [1988], major axis = 4 km, minor axis = 1 km) to a sphere of the same volume and with the same centre depth and pressure change (8 km and 0.5 MPa, respectively) suggests that maximum line-of-sight surface deformation for the ellipsoid is only ~40% that of the sphere. We expect vertically elongated structures, including dykes, persistently open conduits and ellipsoids, to be favored in transtensional or extensional regimes, although the specific geometry of magma storage at any volcano will depend on a combination of both regional and local stress fields. Regional stress in the CAVA is dominated by dextral shear associated with the movement of the fore-arc sliver to the northwest [*Correa-Mora et al*., 2009; *La Femina et al*., 2009; *Alvarado et al*., 2011] and by east-west extension accommodated by north-south trending normal faults (Table 6, comparison to other arc settings). Many magmatic centers in Central America are located in extensional zones (e.g., *Burkart and Self* [1985]). Evidence also suggests that magma reservoirs beneath a number of Central American volcanoes may be vertically elongated (e.g., evidence from polybaric fractionation at San Miguel, El Salvador and narrow reservoir radius at Telica, Nicaragua) [*Carr*, 1981b; *Roche and van Wyk*, 2001].

[46] Despite many significant and comprehensive studies of the geochemistry [e.g., *Carr et al*., 2003; *Bolge et al*., 2009] and tectonics [e.g., *La Femina et al*., 2009; *Alvarado et al*., 2011] of the CAVA, a more complete knowledge of magma storage conditions, including stalling depths, magma reservoir geometries, residence time in the crust, and the exsolved gas content of magma reservoirs is needed to explore the relevance and relative importance of these factors in limiting surface deformation. In combination with deformation measurement, such data have the potential to promote the development of a more systematic understanding of the relationship between magmatic intrusion and crustal deformation.

6. Conclusions

[47] We examine L band InSAR data (2007–2010) for the Central American arc and are able to make measurements at 20 out of 26 historically active volcanoes. We use stacking and time series analysis to distinguish between potential deformation and water vapor artefacts in interferograms and estimate threshold deformation detection rates using time series for the historically active volcanoes (section 2). We find no evidence of magmatic deformation in Central America between 2007 and 2010.

[48] The lack of deformation accompanying explosions at Telica, San Cristóbal, and Poás is unsurprising for such minor eruptions, presumably associated with very small, if any, reservoir volume change or involving little fresh magma (section 4.1). Recent high degassing fluxes and the lack of deformation at Pacaya and Masaya volcanoes suggest that there are no points of localized accumulation of degassed magma at shallow depths (<10 km) in the elastic crust beneath them. This suggests that magma (a) returns to depths below our limits of geodetic detection and/or (b) is dispersed through the crust in multiple smaller intrusions (section 4.2).

[49] Our quantification of detection thresholds for InSAR at Central American volcanoes confirmed a lack of magmatic deformation, found to be statistically significant in relation to the distribution of published magmatic deformation measurements with respect to historically active volcanoes. In spite of high levels of stratified atmospheric water vapor and resulting high threshold for detection (average rate 2.4 cm/yr), we expect the majority of volcano deformation rates measured with InSAR in other parts of the world to have been possible under Central American environmental conditions (section 5). Future analysis of InSAR measurements of volcano deformation will depend on the publication of observations of a lack of deformation, as well as a systematic treatment of the uncertainties associated with InSAR.

[50] We suggest several factors that have the potential to limit magnitudes of surface deformation associated with volcanic activity in Central America (section 5.1). These include deep magma storage and rapid ascent, the potential impact of high parental meltwater content on shallow magma compressibility and the influence of vertically elongated magma reservoir geometries. Such factors may act in isolation or combination to result in reduced magnitudes of surface deformation in Central America relative to other volcanic arcs.

[51] **Acknowledgments.** All ALOS-PALSAR data were acquired through the WInSAR programme at the University of Miami and are copyright of the Japanese Space Agency (JAXA) and the Japanese Ministry of Economy, Trade and Industry (METI). Data were made available by the U.S. Government Research Consortium (USGRC) and the Alaska Satellite Facility (ASF). This work was supported by the National Environmental Research Council through the National Centre for Earth Observation (NCEO), of which the Centre for the Observation and Modeling of Earthquakes, Volcanoes and Tectonics (COMET) is a part. SKE was supported by an NCEO studentship, and JB was funded by the ESA Changing Earth Science Network and a Rosenstiel Postdoctoral Fellowship at the University of Miami. SKE is now supported by the NERC Increasing Resilience to Natural Hazards project: Strengthening Resilience in Volcanic Areas (STREVA). Many thanks to Batuhan Osmanoglu and to Scott Baker for lots of early technical help. This manuscript was improved following insightful reviews by Yosuke Aoki and an anonymous reviewer.

References

Acocella, V., and F. Funiciello (2010), Kinematic setting and structural control of arc volcanism, *Earth Planet. Sci. Lett.*, *289*(12), 43–53, doi:10.1016/j.epsl.2009.10.027.

Agustan, F. Kimata, Y. E. Pamitro, and H. Z. Abidin (2012), Understanding the 2007–2008 eruption of Anak Krakatau Volcano by combining remote sensing technique and seismic data, *Int. J. Appl. Earth Obs. Geoinf.*, *14*, 73–82, doi:10.1016/j.jag.2011.08.011.

Andres, R. J., and A. D. Kasgnoc (1998), A time-averaged inventory of subaerial volcanic sulfur emissions, *J. Geophys. Res.*, *103*(D19), 25251–25, doi:10.1029/98JD02091.

Alvarado, D., C. DeMets, B. Tikoff, D. Hernandez, T. F. Wawrzyniec, C. Pullinger, G. Mattioli, H. L. Turner, M. Rodriguez, and F. Corea-Mora (2011), Forearc motion and deformation between El Salvador and Nicaragua: GPS, seismic, structural, and paleomagnetic observations, *Lithosphere*, *3*(1), 3–21, doi:10.1130/L108.1.

Amelung, F., and S. Day (2002), InSAR observations of the 1995 Fogo, Cape Verde, eruption: Implications for the effects of collapse events upon island volcanoes, *Geophys. Res. Lett.*, *29*(12), 120,000–1, doi:10.1029/2001GL013760.

Amelung, F., S. Jónsson, H. Zebker, and P. Segall (2000), Widespread uplift and 'trapdoor' faulting on Galápagos volcanoes observed with radar interferometry, *Nature*, *407*, 993–996, doi:10.1038/35039604.

Bathke, H., M. Shirzaei, and T. R. Walter (2011), Inflation and deflation at the steep-sided Llaima stratovolcano (Chile) detected by using InSAR, *Geophys. Res. Lett.*, *38*, L10,304, doi:10.1029/2011GL047168.

Berardino, P., G. Fornaro, R. Lanari, and E. Sansosti (2002), A new algorithm for surface deformation monitoring based on small baseline differential SAR interferograms, *IEEE Trans. Geosci. Remote Sens.*, *40*, 2375–2383, doi:10.1109/TGRS.2002.803792.

Biggs, J., T. Wright, Z. Lu, and B. Parsons (2007), Multi-interferogram method for measuring interseismic deformation: Denali fault, Alaska, *Geophys. J. Int.*, *170*, 1165–1179, doi:10.1111/j.1365-246X.2007.03415.x.

Biggs, J., F. Amelung, N. Gourmelen, T. H. Dixon, and S.-W. Kim (2009a), InSAR observations of 2007 Tanzania rifting episode reveal mixed fault and dyke extension in an immature continental rift, *Geophys. J. Int.*, *179*, 549–558, doi:10.1111/j.1365-246X.2009.04262.x.

Biggs, J., E. Y. Anthony, and C. J. Ebinger (2009b), Multiple inflation and deflation events at Kenyan volcanoes, East African Rift, *Geology*, *37*(11), 979–982, doi:10.1130/G30133A.1.

Biggs, J., P. Mothes, M. Ruiz, F. Amelung, T. H. Dixon, S. Baker, and S.-H. Hong (2010), Stratovolcano growth by co-eruptive intrusion: The 2008 eruption of Tungurahua Ecuador, *Geophys. Res. Lett.*, *37*, L21302, doi:10.1029/2010GL044942.

Biggs, J., I. D. Bastow, D. Keir and E. Lewi (2011), Pulses of deformation reveal frequently recurring shallow magmatic activity beneath the Main Ethiopian Rift, *Geochem. Geophys. Geosyst.*, *12*, Q0AB10, doi:10.1029/2011GC003662.

Bolge, L. L., M. J. Carr, K. I. Milidakis, F. N. Lindsay and M. D. Feigenson (2009), Correlating geochemistry, tectonics, and volcanic volume along the Central American volcanic front, *Geochem. Geophys. Geosyst.*, *10*(12), Q12S18, doi:10.1029/2009GC002704.

Bürgmann, R., P. A. Rosen, and E. J. Fielding (2000), Synthetic aperture radar interferometry to measure Earth's surface topography and its deformation, *Annu. Rev. Earth Planet. Sci.*, *28*, 169–209, doi:10.1146/annurev.earth.28.1.169.

Burkart, B., and S. Self (1985), Extension and rotation of crustal blocks in northern Central America and effect on the volcanic arc, *Geology*, *13*, 22–26, doi:10.1130/0091-7613(1985)13<22:EAROCB>2.0.CO;2.

Carr, M. (1981a), Evolution of a young parasitic cone towards a mature central vent; Izalco and Santa Ana volcanoes in El Salvador, Central America, *J. Volcanol. Geotherm. Res.*, *11*, 277–292, doi:10.1016/0377-0273(81)90027-5.

Carr, M. (1981b), Relation of lava compositions to volcano size and structure in El Salvador, *J. Volcanol. Geotherm. Res.*, *10*, 35–48, doi:10.1016/0377-0273(81)90053-6.

Carr, M. (1984), Symmetrical and segmented variation of physical and geochemical characteristics of the Central American volcanic front, *J. Volcanol. Geotherm. Res.*, *20*, 231–252, doi:10.1016/0377-0273(84)90041-6.

Carr, M. J., M. D. Feigenson, L. C. Patino, and J. A. Walker (2003), Volcanism and geochemistry in Central America: Progress and problems, *Geophysical Monograph*, *138*, 153–174, doi:10.1016/0377-0273(84)90041-6.

Cervelli, P., P. Segall, F. Amelung, H. Garbeil, C. Meertens, S. Owen, A. Miklius, and M. Lisowski (2002), The 12 September 1999 Upper East Rift Zone dike intrusion at Kilauea Volcano, Hawaii, *J. Geophys. Res.*, *107*, 2150, doi:10.1029/2001JB000602.

Chaussard, E., and F. Amelung (2012), Precursory inflation of shallow magma reservoirs at west Sunda volcanoes detected by InSAR, *Geophys. Res. Lett.*, *39*, L21311, doi:10.1029/2012GL053817.

Correa-Mora, F., C. DeMets, D. Alvarado, H. L. Turner, G. Mattioli, D. Hernandez, C. Pullinger, M. Rodriguez, and C. Tenorio (2009), GPS-derived coupling estimates for the Central America subduction zone and volcanic arc faults: El Salvador, Honduras and Nicaragua, *Geophys. J. Int.*, *179*(3), 1279–1291, doi:10.1111/j.1365-246X.2009.04371.x.

Duffell, H. J., C. Oppenheimer, D. M. Pyle, B. Galle, A. J. S. McGonigle, and M. R. Burton (2003), Changes in gas composition prior to a minor explosive eruption at Masaya volcano, Nicaragua, *J. Volcanol. Geotherm. Res.*, *126*(3), 327–339, doi:10.1016/S0377-0273(03)00156-2.

Durst, K. S. (2008), Erupted Magma Volume Estimates at Santiaguito and Pacaya Volcanoes, Guatemala using Digital Elevation Models, Master's Thesis, Michigan Technological University.

Dzurisin, D. (2003), A comprehensive approach to monitoring volcano deformation as a window on the eruption cycle, *Rev. Geophys.*, *41*, 1001, doi:10.1029/2001RG000107.

Dzurisin, D., M. Lisowski, C. W. Wicks, M. P. Poland, and E. T. Endo (2006), Geodetic observations and modeling of magmatic inflation at the Three Sisters volcanic center, central Oregon Cascade Range, USA, *J. Volcanol. Geotherm. Res.*, *150*, 35–54, doi:10.1016/j.jvolgeores.2005.07.011.

Ebmeier, S. K., J. Biggs, T. A. Mather, G. Wadge, and F. Amelung (2010), Steady downslope movement on the western flank of Arenal volcano, Costa Rica, *Geochem. Geophys. Geosyst.*, *11*, Q12004, 14PP, doi:10.1029/2010GC003263.

Ebmeier, S. K., J. Biggs, T. A. Mather, J. R. Elliott, G. Wadge, and F. Amelung (2012), Measuring large topographic change with InSAR: Lava thicknesses, extrusion rate and subsidence rate at Santiaguito volcano, Guatemala, *Earth Planet. Sci. Lett.*, *335*, 216225, doi:10.1016/j.epsl.2012.04.027.

Ebmeier, S. K., J. Biggs, T. A. Mather and F. Amelung (2013), Applicability of InSAR to tropical volcanoes: insights from Central America, *Geological Society of London Special Publications*, 380, Remote-sensing of volcanoes and volcanic processes: Integrating observation and modelling, doi:10.1144/SP380.2.

Eggers, A. A. (1983), Temporal gravity and elevation changes at Pacaya volcano, Guatemala, *J. Volcanol. Geotherm. Res.*, *19*(3-4), 223–237, doi:10.1016/0377-0273(83)90111-7.

Elliott, J. R., J. Biggs, B. Parsons and T. J. Wright (2008), InSAR slip rate determination on the Altyn Tagh Fault, northern Tibet, in the presence of topographically correlated atmospheric delays, *Geophys. Res. Lett.*, *35*, 12, doi:10.1016/0377-0273(83)90111-7.

Fisher, R. A. (1922), On the Interpretation of X^2 from Contingency Tables, and the Calculation of P, *J. R. Stat. Soc.*, *85*, 87–94, doi:10.2307/2340521.

Fournier, T. J., M. E. Pritchard, and S. N. Riddick (2010), Duration, magnitude, and frequency of subaerial volcano deformation events: New results from Latin America using InSAR and a global synthesis, *Geochem. Geophys. Geosyst.*, *11*, 1003, doi:10.1029/2009GC002558.

Francis, P., C. Oppenheimer, and D. Stevenson (1993), Endogenous growth of persistently active volcanoes, *Nature*, *366*, 554–557, doi:10.1038/366554a0.

Froger, J., D. Remy, S. Bonvalot, and D. Legrand (2007), Two scales of inflation at Lastarria-Cordon del Azufre volcanic complex, central Andes, revealed from ASAR-ENVISAT interferometric data, *Earth Planet. Sci. Lett.*, *255*, 148–163, doi:10.1016/j.epsl.2006.12.012.

Froger, J.-L., Y. Fukushima, P. Briole, T. Staudacher, T. Souriot, and N. Villeneuve (2004), The deformation field of the August 2003 eruption at Piton de la Fournaise, Reunion Island, mapped by ASAR interferometry, *Geophys. Res. Lett.*, *31*, L14601, doi:10.1029/2004GL020479.

Genco, R. and M. Ripepe (2010), Inflation-deflation cycles revealed by tilt and seismic records at Stromboli volcano, *Geophys. Res. Lett.*, *37*, L12302, doi:10.1029/2010GL042925.

Goldstein, R. M., H. A. Zebker, and C. L. Werner (1988), Satellite radar interferometry—Two-dimensional phase unwrapping, *Radio Sci.*, *23*, 713–720, doi:10.1029/RS023i004p00713.

Harris, A. J. L., L. P. Flynn, D. A. Rothery, C. Oppenheimer, and S. B. Sherman (1999), Mass flux measurements at active lava lakes: Implications for magma recycling, *J. Geophys. Res.*, *104*, 7117–7136, doi:10.1029/98JB02731.

Heleno, S. I. N., C. Frischknecht, N. d'Oreye, J. N. P. Lima, B. Faria, R. Wall, and F. Kervyn (2010), Seasonal tropospheric influence on SAR interferograms near the ITCZ—The case of Fogo Volcano and Mount Cameroon, *J. Afr. Earth Sci.*, *58*, 833–856, doi:10.1016/j.jafrearsci.2009.07.013.

Johnson, D. J., F. Sigmundsson, and P. T. Delaney (2000), Comment on "Volume of magma accumulation or withdrawal estimated from surface uplift or subsidence, with application to the 1960 collapse of Klauea volcano" by P. T. Delaney and D. F. Mctigue, *Bull. Volcanol.*, *61*, 491–493, doi:10.1007/s004450050006.

Kazahaya, K., H. Shinohara, and G. Saito (1994), Excessive degassing of Izu-Oshima volcano: magma convection in a conduit, *Bull. Volcanol.*, *56*, 207–216, doi:10.1007/BF00279605.

La Femina, P. C., C. B. Connor, B. E. Hill, W. Strauch, and J. A. Saballos (2009), Fore-arc motion and Cocos Ridge collision in Central America, *Geochem. Geophys. Geosyst.*, *10*, Q05S14, doi:10.1029/2008GC002181.

Lanari, R., G. De Natale, P. Berardino, E. Sansosti, G. P. Ricciardi, S. Borgstrom, P. Capuano, F. Pingue, and C. Troise (2002), Evidence for a peculiar style of ground deformation inferred at Vesuvius volcano, *Geophys. Res. Lett.*, *29*(9), 1292, doi:10.1029/2001GL014571.

Locke, C. A., H. Rymer, and J. Cassidy (2003), Magma transfer processes at persistently active volcanoes: insights from gravity observations, *J. Volcanol. Geotherm. Res.*, *127*, 73–86, doi:10.1016/S0377-0273(03)00179-3.

Lu, Z. (2007), InSAR Imaging of Volcanic Deformation over Cloud-prone Areas-Aleutian Islands, *Photogramm. Eng. Remote Sens.*, *73*, 245–257.

Lu, Z., and D. Dzurisin (2010), Ground surface deformation patterns, magma supply, and magma storage at Okmok volcano, Alaska, from InSAR analysis: 2. Coeruptive deflation, July–August 2008, *J. Geophys. Res.*, *115*, B14–B00B03, doi:10.1029/2009JB006970.

Lu, Z., and J. T. Freymueller (1998), Synthetic aperture radar interferometry coherence analysis over Katmai volcano group, Alaska, *J. Geophys. Res.*, *103*, 29,887–29,894, doi:10.1029/98JB02410.

Lu, Z., T. Masterlark, J. Power, D. Dzurisin, and C. Wicks (2002a), Subsidence at Kiska Volcano, Western Aleutians, detected by satellite radar interferometry, *Geophys. Res. Lett.*, *29*(18), 1855, doi:10.1029/2002GL014948.

Lu, Z., J. A. Power, V. S. McConnell, C. Wicks, and D. Dzurisin (2002b), Preeruptive inflation and surface interferometric coherence characteristics revealed by satellite radar interferometry at Makushin Volcano, Alaska: 1993–2000, *J. Geophys. Res.*, *107*(B11), 2266, doi:10.1029/2001JB000970.

Lu, Z., D. Wicks, D. Dzurisin, J. Power, W. Tatcher, and T. Masterlark (2003), Interferometric synthetic aperture radar studies of Alaska volcanoes, *EOM*, *12*, 8–18.

Lundgren, P., and Z. Lu (2006), Inflation model of Uzon caldera, Kamchatka, constrained by satellite radar interferometry observations, *Geophys. Res. Lett.*, *33*, L06301, doi:10.1029/2005GL025181.

Lundgren, P., S. Usai, E. Sansosti, R. Lanari, M. Tesauro, G. Fornaro, and P. Berardino (2001), Modeling surface deformation observed with synthetic aperture radar interferometry at Campi Flegrei caldera, *J. Geophys. Res.*, *106*, 19,355–19,366, doi:10.1029/2001JB000194.

Lundgren, P., P. Berardino, M. Coltelli, G. Fornaro, R. Lanari, G. Puglisi, E. Sansosti, and M. Tesauro (2003), Coupled magma chamber inflation and sector collapse slip observed with synthetic aperture radar interferometry on Mt. Etna volcano, *J. Geophys. Res.*, *108*(B5), 2247, doi:10.1029/2001JB000657.

Lyons, J., G. Whaite, M. Ichihara and J. Lees (2012), Tilt prior to explosions and the effect of topography on ultra-long-period seismic records at Fuego volcano, Guatemala, *Geophys. Res. Lett.*, *39*, L08305, doi:10.1029/2012GL051184.

Martini, F., F. Tassi, O. Vaselli, R. Del Potro, M. Martinez, R. van der Laat, and E. Fernandez (2010), Geophysical, geochemical and geodetical signals of reawakening at Turrialba volcano (Costa Rica) after almost 150 years of quiescence, *198*(2), 416–432, doi:10.1016/j.jvolgeores.2010.09.021.

Massonnet, D., and K. L. Feigl (1995), Discrimination of geophysical phenomena in satellite radar interferograms, *Geophys. Res. Lett.*, *22*, 1537–1540, doi:10.1029/95GL00711.

Massonnet, D., and K. L. Feigl (1998), Radar interferometry and its application to changes in the Earth's surface, *Rev. Geophys.*, *36*, 441–500, doi:10.1029/97RG03139.

Masterlark, T., and Z. Lu (2004), Transient volcano deformation sources imaged with interferometric synthetic aperture radar: Application to Seguam Island, Alaska, *J. Geophys. Res.*, *109*(B18), B01401, doi:10.1029/2003JB002568.

Mastin, L. G., E. Roeloffs, N. M. Beeler, and J. E. Quick (2008), Constraints on the size, overpressure, and volatile content of the Mount St Helen's magma system from geodetic and dome-growth measurements during the 2004–2006 eruption, *USGS Prof. Pap.*, *1750*, 461–488.

Mastin, L. G., M. Lisowski, E. Roeloffs, and N. Beeler (2009), Improved constraints on the estimated size and volatile content of the Mount St. Helens magma system from the 2004–2008 history of dome growth and deformation, *Geophys. Res. Lett.*, *36*, L20304, doi:10.1029/2009GL039863.

Mather, T. A., D. M. Pyle, V. I. Tsanev, A. J. S. McGonigle, C. Oppenheimer, and A. G. Allen (2006), A reassessment of current volcanic emissions from the Central American arc with specific examples from Nicaragua, *J. Volcanol. Geotherm. Res.*, *149*, 297–311, doi:10.1016/j.jvolgeores.2005.07.021.

Mogi, K. (1958), Relations between the Eruption of various volcanoes and the Deformations of the Ground Surfaces around them, *Bull. Earthquake Res. Inst.*, *36*, 99–134.

Moran, S. C., O. Kwoun, T. Masterlark, and Z. Lu (2006), On the absence of InSAR-detected volcano deformation spanning the 1995 1996 and 1999 eruptions of Shishaldin Volcano, Alaska, *J. Volcanol. Geotherm. Res.*, *150*, 119–131, doi:10.1016/j.jvolgeores.2005.07.013.

Mothes, P., J. Biggs, S. Baker, S. Hong, F. Amelung, and T. Dixon (2008), Survey of volcanic activity in Ecuador using L-band SAR, *AGU Fall Meeting Abstract.*

Ofeigsson, B., A. Hooper, F. Sigmundsson, E. Sturkell, and R. Grapenthin (2011), Deep magma storage at Hekla volcano, Iceland, revealed by InSAR time series analysis, *J. Geophys. Res.*, *116*(B5), B05,401, doi:10.1029/2010JB007576.

Parks, M., J. Biggs, P. England, T. A. Mather, P. Nomikou, K. Palamartchouk, X. Papanikolaou, and D. Paradissis (2012), Evolution of Santorini Volcano dominated by episodic and rapid fluxes of melt from depth, *Nat. Geosci.*, *5*(10), 749–754, doi:10.1038/ngeo1562.

Parks, M. M., J. Biggs, T. A. Mather, D. M. Pyle, F. Amelung, M. Monsalve, and L. N. Medina (2011), Co-eruptive subsidence at Galeras identified during an Insar survey of Colombian volcanoes (2006–2009), *J. Volcanol. Geotherm. Res.*, *202*(3-4), 228–240, doi:10.1016/j.jvolgeores.2011.02.007.

Patino, L. C., M. J. Carr, and M. D. Feigenson (2000), Local and regional variations in Central American arc lavas controlled by variations in subducted sediment input, *Contrib. Mineral. Petrol.*, *138*(3), 265–283, doi:10.1007/s004100050562.

Pavez, A., D. Remy, S. Bonvalot, M. Diament, G. Gabalda, J.-L. Froger, P. Julien, D. Legrand, and D. Moisset (2006), Insight into ground deformations at Lascar volcano (Chile) from SAR interferometry, photogrammetry and GPS data: Implications on volcano dynamics and future space monitoring, *Remote Sens. Environ.*, *100*(3), 307–320, doi:10.1016/j.rse.2005.10.013.

Pertermann, M., and C. C. Lundstrom (2006), Phase equilibrium experiments at 0.5 GPa and 1100 1300 °C on a basaltic andesite from Arenal volcano, Costa Rica, *J. Volcanol. Geotherm. Res.*, *157*, 222–235, doi:10.1016/j.jvolgeores.2006.03.043.

Philibosian, B., and M. Simons (2011), A survey of volcanic deformation on Java using ALOS PALSAR interferometric time series, *Geochem. Geophys. Geosyst.*, *12*, Q11004, doi:10.1029/2011GC003775.

Pinel, V., A. Hooper, S. de La Cruz-Reyna, G. Reyes-Davila, M. P. Doin, and P. Bascou (2011), The challenging retrieval of the displacement field from InSAR data for andesitic stratovolcanoes: Case study of Popocatepetl and Colima Volcano, Mexico, *J. Volcanol. Geotherm. Res.*, *200*, 49–61, doi:10.1016/j.jvolgeores.2010.12.002.

Poland, M., G. Bawden, M. Lisowski, and D. Dzurisin (2004), Newly discovered subsidence at Lassen Peak, southern Cascade Range, California, from InSAR and GPS, *AGU Fall Meeting Abstract*, *G51A-0068*.

Poland, M., R. Bürgmann, D. Dzurisin, M. Lisowski, T. Masterlark, S. Owen, and J. Fink (2006), Constraints on the mechanism of long-term, steady subsidence at Medicine Lake volcano, northern California, from GPS, leveling, and InSAR, *J. Volcanol. Geotherm. Res.*, *150*, 55–78, doi:10.1016/j.jvolgeores.2005.07.007.

Pritchard, M. E., and M. Simons (2004a), An InSAR-based survey of volcanic deformation in the central Andes, *Geochem. Geophys. Geosyst.*, *5*, 2002, doi:10.1029/2003GC000610.

Pritchard, M. E., and M. Simons (2004b), An InSAR-based survey of volcanic deformation in the southern Andes, *Geophys. Res. Lett.*, *31*, L15,610, doi:10.1029/2004GL020545.

Remy, D., S. Bonvalot, P. Briole, and M. Murakami (2003), Accurate measurements of tropospheric effects in volcanic areas from SAR interferometry data: Application to Sakurajima volcano (Japan), *Earth Planet. Sci. Lett.*, *213*, 299–310, doi:10.1016/S0012-821X(03)00331-5.

Roche, O., B. van Wyk de Vries, and T. Druitt (2001), Sub-surface structures and collapse mechanisms of summit pit craters, *J. Volcanol. Geotherm. Res.*, *105*, 1–18, doi:10.1016/S0377-0273(00)00248-1.

Roggensack, K., R. L. Hervig, S. B. McKnight, and S. N. Williams (1997), Explosive basaltic volcanism from Cerro Negro volcano: Influence of volatiles on eruptive style, *Science*, *277*, 1639–1642, doi:10.1126/science.277.5332.1639.

Rose, W. I. (1972), Notes on the 1902 eruption of Santa María volcano, Guatemala, *Bull. Volcanol.*, *36*, 29–45, doi:10.1007/BF02596981.

Rosen, P. A., S. Hensley, G. Peltzer, and M. Simons (2004), Updated repeat orbit interferometry package released, *Eos Transactions*, *AGU*, *85*(5), 47, doi:10.1029/2004EO050004.

Ruch, J., J. Anderssohn, T. R. Walter, and M. Motagh (2008), Caldera-scale inflation of the Lazufre volcanic area, South America: Evidence from InSAR, *J. Volcanol. Geotherm. Res.*, *174*, 337–344, doi:10.1016/j.jvolgeores.2008.03.009.

Rymer, H., J. Cassidy, C. A. Locke, and J. B. Murray (1995), Magma movements in Etna volcano associated with the major 1991 1993 lava eruption: Evidence from gravity and deformation, *Bull. Volcanol.*, *57*, 451–461, doi:10.1007/BF00300989.

Sadofsky, S. J., M. Portnyagin, K. Hoernle, and P. van den Bogaard (2008), Subduction cycling of volatiles and trace elements through the Central American volcanic arc: Evidence from melt inclusions, *Contrib. Mineral. Petrol.*, *155*, 433–456, doi:10.1007/s00410-007-0251-3.

Sanderson, R. W., J. B. Johnson, and J. M. Lees (2010), Ultra-long period seismic signals and cyclic deflation coincident with eruptions at Santiaguito volcano, Guatemala, *J. Volcanol. Geotherm. Res.*, *198*, 35–44, doi:10.1016/j.jvolgeores.2010.08.007.

Sigmundsson, F., P. Durand, and D. Massonnet (1999), Opening of an eruptive fissure and seaward displacement at Piton de la Fournaise volcano measured by RADARSAT satellite radar interferometry, *Geophys. Res. Lett.*, *26*, 533–536, doi:10.1029/1999GL900055.

Sigmundsson, F. et al. (2010), Intrusion triggering of the 2010 Eyjafjallajökull explosive eruption, *Nature*, *468*, 426–430, doi:10.1038/nature09558.

Smithsonian Institution (1993a), Poás, *Bulletin of the Global Volcanism Network*, *18*(1).

Smithsonian Institution (1993b), Poás, *Bulletin of the Global Volcanism Network*, *18*(3).

Smithsonian Institution (1993c), Irazú , *Bulletin of the Global Volcanism Network*, *18*(1).

Smithsonian Institution (2000), Poás, *Bulletin of the Global Volcanism Network*, *25*(8).

Smithsonian Institution (2008), Turrialba, *Bulletin of the Global Volcanism Network*, *33*(1).

Smithsonian Institution (2009), Masaya, *Bulletin of the Global Volcanism Network*, *34*(3).

Sparks, R. S. J., C. B. Folkes, M. C. Humphreys, D. N. Barfod, J. Clavero, M. C. Sunagua, S. R. McNutt, and M. E. Pritchard (2008), Uturuncu volcano, Bolivia: Volcanic unrest due to mid-crustal magma intrusion, *Am. J. Sci.*, *308*(6), 727–769, doi:10.2475/06.2008.01.

Stoiber, R. E., S. N. Williams, and B. J. Huebert (1986), Sulfur and halogen gases at Masaya Caldera complex, Nicaragua: Total flux and variations with time, *J. Geol. Res.*, *91*, 12,215–12,232, doi:10.1029/JB091iB12p12215.

Sykioti, O., C. C. Kontoes, P. Elias, P. Briole, M. Sachpazi, D. Paradissis, and I. Kotsis (2003), Ground deformation at Nisyros volcano (Greece) detected by ERS-2 SAR differential interferometry, *Int. J. Remote Sens.*, *24*, 183–188, doi:10.1080/01431160305000.

Syracuse, E. M., P. E. van Keken, and G. A. Abers (2010), The global range of subduction zone thermal models, *Phys. Earth Planet. Inter.*, *183*, 73–90, doi:10.1016/j.pepi.2010.02.004.

van Keken, P. E., B. R. Hacker, E. M. Syracuse, and G. A. Abers (2011), Subduction factory: 4. Depth-dependent flux of H_2O from subducting slabs worldwide, *J. Geophys. Res.*, *116*, B01401, doi:10.1029/2010JB007922.

Venzke, E., R. W. Wunderman, L. McClelland, T. Simkin, J. F. Luhr, L. Siebert, G. Mayberry and S. Sennart (2002), Global Volcanism, 1968 to the Present, *Smithsonian Institution*, *Global Volcanism Program Digital Information Series*, *GVP-4*, http://www.volcano.si.edu/reports/.

Voight, B., R. S. J. Sparks, A. S. Miller, et al. (1999), Magma flow instability and cyclic activity at Soufriere Hills Volcano, Montserrat, British West Indies, *Science*, *283*, 5405,1138–1142, doi:10.1126/science.283.5405.1138.

Wadge, G., G. S. Mattioli, and R. A. Herd (2006), Ground deformation at Soufrière Hills Volcano, Montserrat during 1998–2000 measured by radar interferometry and GPS, *J. Volcanol. Geotherm. Res.*, *152*, 157–173, doi:10.1016/j.jvolgeores.2005.11.007.

Walker, J. A. (1993), Shallow open-system evolution of basaltic magma beneath a subduction zone volcano: The Masaya Caldera Complex, Nicaragua, *J. Volcanol. Geotherm. Res.*, *56*, 379–400, doi:10.1016/0377-0273(93)90004-B.

Walker, J. A., K. Roggensack, L. C. Patino, B. I. Cameron, and O. Matías (2003), The water and trace element contents of melt inclusions across an active subduction zone, *Contrib. Mineral. Petrol.*, *146*, 62–77, doi:10.1007/s00410-003-0482-x.

Wallace, P. J. (2005), Volatiles in subduction zone magmas: Concentrations and fluxes based on melt inclusion and volcanic gas data, *J. Volcanol. Geotherm. Res.*, *140*, 217–240, doi:10.1016/j.jvolgeores.2004.07.023.

Watson, I. M. et al. (2000), The relationship between degassing and ground deformation at Soufriére Hills Volcano, Montserrat, *J. Volcanol. Geotherm. Res.*, *98*, 117–126, doi:10.1016/S0377-0273(99)00187-0.

Wauthier, C., W. Cayol, F. Kervyn, and N. d'Oreye (2009), The January 2002 eruption of Nyiragongo Volcano (DRC) captured by InSAR, in *Geoscience and Remote Sensing Symposium*, *2009 IEEE International*, *IGARSS 2009*, vol. 2, pp. II-416–II-419, doi:10.1109/IGARSS.2009.5418103.

Wauthier, C., V. Cayol, F. Kervyn, and N. d'Oreye (2012), Magma sources involved in the 2002 Nyiragongo eruption, as inferred from an InSAR analysis, *J. Geophys. Res.*, *117*, B05,411, doi:10.1029/2011JB008257.

Williams-Jones, G., H. Rymer, and D. A. Rothery (2003), Gravity changes and passive SO_2 degassing at the Masaya caldera complex, Nicaragua, *J. Volcanol. Geotherm. Res.*, *123*, 137–160, doi:10.1016/S0377-0273(03)00033-7.

Witter, M. et al. (2011), May 2011 eruption of Telica Volcano, Nicaragua: Multidisciplinary observations, *America Geophysical Union Fall Meeting Abstract*, *V53E-2670*, San Francisco 5-9 Dec.

Yang, X.-M., P. M. Davis, and J. H. Dieterich (1988), Deformation from inflation of a dipping finite prolate spheroid in an elastic half-space as a model for volcanic stressing, *J. Geophys. Res.*, *93*, 4249–4257, doi:10.1029/JB093iB05p04249.

Zebker, H. A., F. Amelung, and S. Jonsson (2000), Remote sensing of volcano surface and internal processes using radar interferometry, *Geophys. Monogr.*, *116*, 179–205.

Zellmer, G. F. (2008), Some first order observations on magma transfer from mantle wedge to upper crust at arc volcanoes, vol. 304, Geological Society, London, Special Publications, doi:10.1144/SP304.1.

Zimmer, M. M., T. P. Fischer, D. R. Hilton, G. E. Alvarado, Z. D. Sharpe and J. A. Walker (2004), Nitrogen systematics and gas fluxes of subduction zones: Insights from Costa Rica arc volatiles, *Geochem. Geophys. Geosyst.*, *5*(5), Q05J11, doi:10.1029/2003GC000651.